AD-A120 728 HIGH-SPEED SCAN ROTATING MIRRORS FOR HIGH ENERGY LASER SYSTEMS(U) FOREIGN TECHNOLOGY DIV WRIGHT-PATTERSON AFB OH S HU 22 SEP 82 FTD-ID(RS)T-0774-82 1/1

UNCLASSIFIED F/G 20/5 NL

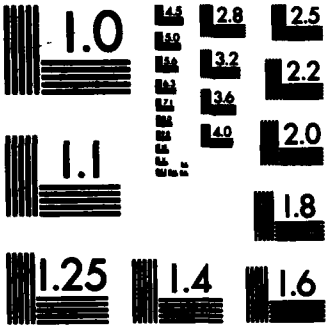

MICROCOPY RESOLUTION TEST CHART
NATIONAL BUREAU OF STANDARDS-1963-A

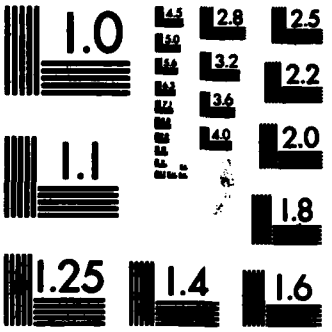

MICROCOPY RESOLUTION TEST CHART
NATIONAL BUREAU OF STANDARDS-1963-A

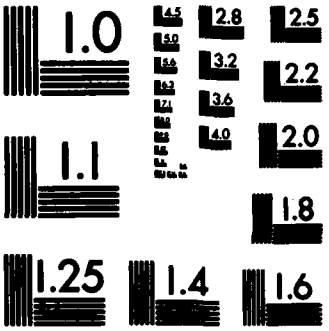

MICROCOPY RESOLUTION TEST CHART
NATIONAL BUREAU OF STANDARDS-1963-A

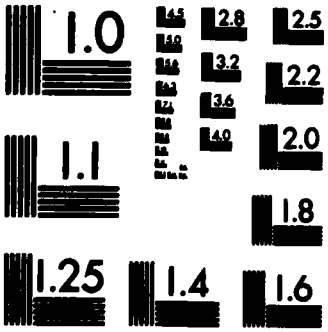

MICROCOPY RESOLUTION TEST CHART
NATIONAL BUREAU OF STANDARDS-1963-A

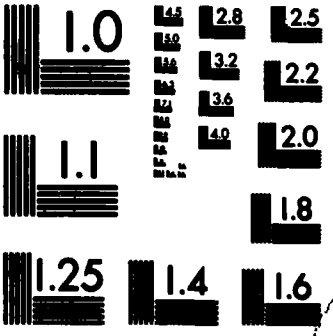

MICROCOPY RESOLUTION TEST CHART
NATIONAL BUREAU OF STANDARDS-1963-A

FTD-ID(RS)T-0774-82

FOREIGN TECHNOLOGY DIVISION

HIGH-SPEED SCAN ROTATING MIRRORS FOR HIGH ENERGY LASER SYSTEMS

by

Hu Shaoyi

EDITED TRANSLATION

FTD-ID(RS)T-0774-82 22 September 1982

MICROFICHE NR: FTD-82-C-001253

HIGH-SPEED SCAN ROTATING MIRRORS FOR HIGH ENERGY LASER SYSTEMS

By: Hu Shaoyi

English pages: 13

Source: Jiguang, Vol. 7, Nr. 12, 1980, pp. 27-31; 26

Country of origin: China
Translated by: LEO KANNER ASSOCIATES
F33657-81-D-0264
Requester: FTD/TQTD

PREPARED BY:

TRANSLATION DIVISION
FOREIGN TECHNOLOGY DIVISION
WP-AFB, OHIO.

GRAPHICS DISCLAIMER

All figures, graphics, tables, equations, etc. merged into this translation were extracted from the best quality copy available.

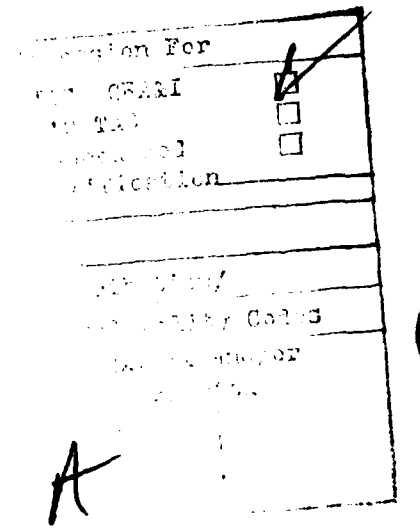

HIGH-SPEED SCAN ROTATING MIRRORS FOR HIGH ENERGY LASER SYSTEMS

Hu Shaoyi
Shanghai Institute of Optics and Fine Mechanics, Chinese Academy of Sciences
Submitted 19 November 1979

Two types of periodic scan rotating mirrors used in high energy laser systems are introduced. Both rotating mirrors are driven by air turbines: one of them is supported by a hydrostatic gas bearing while the other is supported by three holding wheels centerlessly. In this paper their design, fabrication and experimental results are described.

When a high brightness laser beam passes through a series of magnifiers in a high energy Nd glass laser device, there are local temperature differences in the working medium due to the uneven laser energy field; these temperature differences lead to differences in thermal deformation, diffusion, deterioration of laser beam orientation, and lowering of laser brightness.

It is proven to be effective by using the scan light beam method in order to reduce as much as possible the effect on light beam orientation by diffusion phenomenon. The concept of the method is to artificially disturb the light beam direction in the working medium in order to reduce differences of thermal deformation in the local zones. The key to success and failure of the experiment is the requirement of a large-diameter, high r.p.m. and high stability scan rotating

mirror, which is to scan, in a certain form, the laser beam entering the magnifier series; in addition, the wider laser beam as the output from the magnifier series is again restored by the rotating mirror to a slender light beam as the output. The schematic diagram of the working principle is shown in Fig. 1. According to different cross sections of the magnifier, there are also two kinds of shapes for the rotating mirror: (1) Ring-shaped scan rotating mirror (for use in rod-shaped amplifier) and (2) Matrix-shaped scan rotating mirror, an umbrella-shaped rotating mirror (for use in sheet-shaped magnifier). The structural designs of these two kinds of rotating mirrors are described in the following:

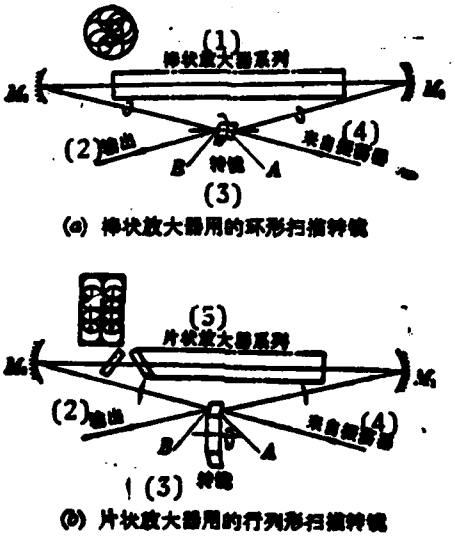

(a) 棒状放大器用的环形扫描转镜

(b) 片状放大器用的行列形扫描转镜

Fig. 1. Schematic diagram of light channels (M_1 and M_2 are reflective mirrors): (a) Ring-shaped scan rotating mirror used for rod-shaped magnifier; (b) Matrix-shaped scan rotating mirror used for sheet-shaped magnifier. Key: (1) Rod-shaped magnifier series; (2) Output; (3) Rotating mirror; (4) From oscillator; (5) Sheet-shaped magnifier series.

I. Ring-shaped Scan Rotating Mirror

Fig. 1(a) shows this kind of rotating mirror, which scans the light beam in a ring shape. The working principle of the rotating mirror is similar to the conventional twisting mirror; that is, the normal of the mirror surface forms an angle with the rotating axis. When the mirror blade rotates around its axis, the incident light beam with a certain incident angle displays a conic-shape scanning its light axis after the light beam was reflected from the mirror surface. It differs from the twisting mirror in that the ring-shaped light beam following magnification should again pass through the back surface B of the same rotating mirror for restoration. In order to require that the light beam scans at high speed and restores without distortion to a laser beam as output, a very high degree of parallelism is required between mirror surfaces A and B. In addition, there should be a very high stability between these two mirror surfaces during high-speed rotation. This stability requirement can be met only by making these two mirror surfaces as both sides of a single mirror plate and the parallelism (less than or equal to 5" of allowance for deviation from the parallelism) while using a super-precision optical processing technique. Some degree of difficulty is brought to the design of the mechanical structure in requiring both sides of a mirror plate to be useful with a relatively large light aperture of ϕ50 mm and very high rotating speed n=30,000~40,000 r.p.m. (corresponding to more than 5 scans in 10 milliseconds). First, the problem of selecting a bearing should be solved. Under the conditions of relatively large shaft neck (D>60 mm) and very high rotating speed (Dn>2,000,000), the conventional roller bearing and slide bearing (oil-film bearing) are obviously not satisfactory for this purpose. Only the hydrostatic gas bearing is the most ideal because the bearing has characteristics of low friction, good stability, and long service life. The author selected the hydrostatic gas bearing for this kind of rotating mirror. Next in order of importance is selection of power to operate the experimental devices. To suit this purpose, the power device should have a compact structure, short starting time, and high adaptability. Therefore, the author selected an air turbine to drive the rotating mirror. Figure 2 shows the structural diagram of the ring-shaped scan rotating mirror.

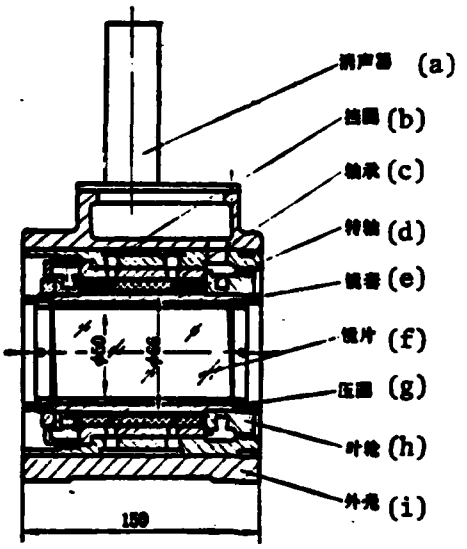

Fig. 2. Structural diagram of 40,000 r.p.m. high-speed rotating mirror. Key: (a) Silencer; (b) Shield winding; (c) Bearing; (d) Rotating shaft; (e) Mirror sleeve; (f) Mirror plate; (g) Pressure winding; (h) Blade wheel; (i) Outer shell.

1. Design of hydrostatic gas bearing

(1) Determination of bearing parameters: based on the diameter of the light beam to be scanned, the outer diameter, ϕ66 mm, of the mirror frame is adopted as the neck diameter of the rotating shaft; the overall length of the bearing is L=70 mm; and a double-row (six holes evenly distributed in each row) capillary nozzle arrangement is selected for the bearing, as shown in Fig. 3. From the well-known gas-film bearing calculation formula,

$$F_0 = \sqrt{\frac{K-1}{2K_0RT_0}} \times \frac{P_0 D}{144\mu O_d} \times \frac{h^3}{(L/2)d} \qquad (1)$$

In the equation, R is the air constant; μ is the absolute viscosity of air; C_d is the exhaust coefficient, generally at 0.9; T_s is the absolute temperature; K is the value of specific heat of the gas; g is the gravitational acceleration; P_s

is the inlet gas pressure; D is the bearing diameter; L/2 is bearing half length; h is clearance, d is diameter of capillary nozzles; and F_0 is the dimensionless parameter, which is determined to be 0.4 from the experimental curve. By substituting all known values, we derive the relationship equation among the three: P_s (kg/cm^2), h (cm) and d (cm)

$$1034.[(P_s h^2)/d]=0.4 \qquad (2)$$

We can see from the equation that P_s, h and d can be arbitrarily selected within a wide range. As proven by experience, after the value of P_s is determined, if values of h and d are selected to be too large, the stability and rigidity of the shaft will be reduced. If d<0.3 mm, not only is the processing more difficult but also breakdowns due to plugging of capillary nozzles and overloading cap shaft will develop when the air purity is not high. So, consideration is given to the design characteristics of light loading and high speed. Finally, P_s was selected as 1.7 kg/cm^2 and d=0.4 mm; upon calculation, h≈0.030 mm (which means that the matching clearance between the bearing hole and diameter is 0.060 mm).

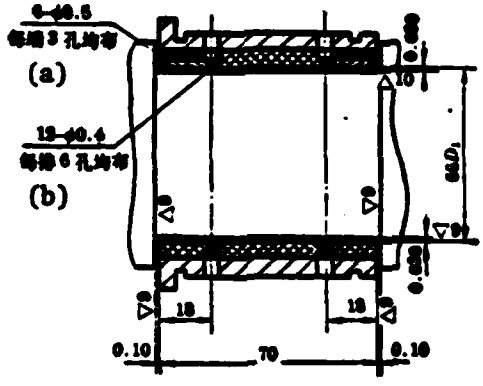

Fig. 3. Structural diagram of gas-film bearing. Key: (a) Three holes evenly distributed at each terminal; (b) Six holes evenly distributed in each row.

In order to prevent lengthwide motion of the rotating-mirror shaft, a two-plane stop-push gas-film bearing was designed by using two ends of the shaft and the space between shoulders of the rotating shaft (Fig. 3). The parameters are d'=0.5 mm (three holes evenly distributed at each end) and h'=0.10 mm.

(2) Selection of materials: A two-layer structure is used for the bearing. The outer-sleeve is made of aluminum bronze ZQA19-4, which is high in strength and has desirable anti-corrosion characteristics. The material for the inner sleeve is the electrochemical graphite DM4, which has the characteristics of good anti-sticking viscosity and grinding resistance. The material is, by itself, a good solid lubricant, since it can prevent those undesirable phenomena of sticking to the shaft and rough scratching on the surface of the shaft neck due to occasional collision abrasion during starting or high-speed rotation of the mirror.

The material for the rotating shaft is stainless steel 4Cr13; the surface hardness should be $H_{RC}\geq 55$ after heat treatment. The outer circle of the shaft should be precisely ground to over ∇10; the clearance between the shaft hole diameter and the shaft is $0.060^{+0.005}$ mm.

2. Design of blade wheel of air turbine

A remodeled impact type turbine blade wheel is selected because of the simplicity in the manufacturing technique of the blade wheel and under conditions allowing proper reduction of efficiency to some extent. The main characteristic of the blade wheel is that the position of the nozzle is perpendicular to the main rotating shaft, as shown in Fig. 4. The parameters of the blade wheel can be designed and determined by the use of the classical calculation formula for impact type blade wheels (the calculation is omitted here). Finally, the parameters of the blade wheel are determined as follows:

Assuming that the diameter of the nozzle ring (D=90 mm) and blade-wheel diameter D_0=89.9 mm; blade number Z=18 and θ=20°, then the maximum height of the blade: $h=(D_0/2)(1-\cos\theta)\approx 2.6$ mm.

The distance (between the nozzle and the shaft line of rotation) $H=(D_0/2)-(h/2)$ =43.6 mm. The tangent angle (between the nozzle central line and the wheel circumference) $\alpha_1=\cos^{-1}(2H/D_0)\approx 14°$.

We assume that the blade width B=10.5 mm, arc radius R=6 mm, B_1=2 mm, nozzle diameter d=1 mm, and nozzle number n=6.

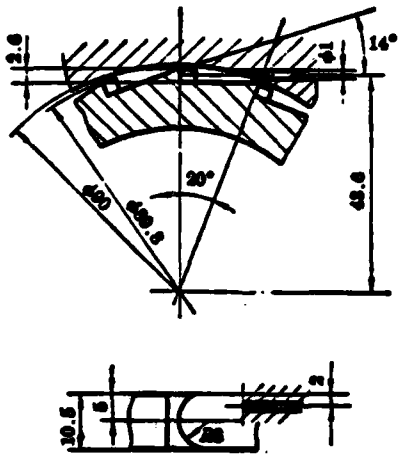

Fig. 4. Blade wheel and nozzle of a 40,000 r.p.m. rotating mirror.

The blade wheel is made by milling super-hard aluminum LC-4. The blade wheel and the rotating shaft are fitted into one piece by use of thermal shrink fitting. The rotating shaft (after being fitted with optical elements) is tested for dynamic equilibrium on a highly precise dynamic equilibrium testing machine. It is required that the dynamic equilibrium precision be less than 0.5 micron.

The calculated inlet gas pressure is 6.5 kg/cm^2 (absolute pressure) and the rated rotating speed (in design) is 40,000 r.p.m.

II. Matrix-shaped Scan Rotating Mirror

Figure 1(b) shows this kind of rotating mirror, which scans the light beam in a matrix shape and restores the beam; in other words, the circular light beam is formed into a rectangular, or nearly rectangular, shape. By magnification with use of a sheet-shaped magnifier, again the same rotating mirror is used to restore the light beam to the single beam circular shape as output. We adopted the umbrella-shaped scan mirror. Based on the predetermined number of rows to be scanned, the number of pieces in each group of mirror plates can be determined. From a disk of an umbrella-shaped rotating mirror composed of several groups in cyclic arrangement, several scans are performed for each rotation. The surface A

of the mirror is the scan mirror surface, and the surface B is the restored mirror surface. The working principle of the scan (see Fig. 5) and main parameters of the mirror plate are determined as follows:

β -- the included angle between the normal of the reflecting surface of the mirror plate, and the shaft line of the scan mirror rotation;

α -- the scan angle (scan field angle) $\alpha=(h/\ell^*_{max})$. h is the height of the last working medium; ℓ^*_{max} is the distance from the last piece of working medium to the scan mirror. $\ell^*_{max}=\ell_{air}+(\ell_{glass}/n_{glass})$; and

γ -- the field angle ($\gamma=(B/R)$) between the scan mirror center to the mirror-plate thickness. B is the width of the mirror plate and R is the radius of the scan mirror.

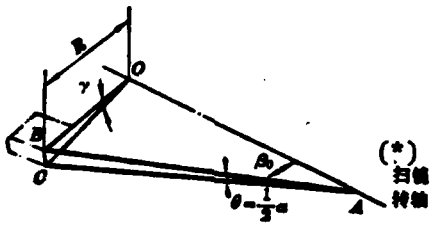

Fig. 5. Diagram showing the scan principle of the umbrella-shaped rotating mirror.
Key: (*) Rotating shaft of scan mirror.

The value of β can be determined by the relationship of the three. When the scan mirror is turned by an angle γ (in radians), it is required that the light beam scan an angle α (in radians); that is, the mirror surface deflects $(1/2)\alpha$ radians. The relationship of the three is:

$$\sin\beta_0=\frac{\sin\frac{\alpha}{2}}{\sin\frac{\gamma}{2}}$$

In the equation, β_0 is the value of β of the reflective mirror corresponding to the central line. If the scan is conducted on several rows, it is required that two adjacent light beams can be separated when the scan light beam reaches

working medium. In order to meet this requirement, the angle β of a rror plates should be, respectively, β_1, β_2, β_3, ...; and the difference of two adjacent mirror plates should be δ_o. If the number of mirror a odd number for a particular group, then $\beta=\beta_o$ for the middle mirror two adjacent mirror plates, the difference values are, respectively, $\cdot\delta_o$.

assumed that the diameter of the scan light beam is ϕ60 mm, the required cans is 10 within a period of 10 milliseconds, and the light aperture stage sheet-shaped magnifier is 300x120 mm, $\ell^*_{max}\approx 9\sim 10$ meters. If two as are performed and the outer diameter of the mirror plate is ϕ210 mm re altogether 16 pieces of mirror plates (two pieces in a group, totaling the shape of the mirror is shown in Fig. 6. After simple calculation, ers of the scan mirror are as follows:

$$\gamma_1 = 27°8' \qquad \gamma_2 = 17°52'$$
$$\beta_1 = 55' \qquad \beta_2 = 62'$$

g speed $n=10^3 x(60/8)=7500$ r.p.m.

cation of mirror plate: Consideration is given that both surfaces of ate are used for light reflection and their dynamic precision should be therefore, the method of mirror plate fixation used in the design is external cylindrical surface of the mirror plate on the inner wall of oop ring (mirror ring) with sufficient rigidity. The inner cylindrical the mirror plate is in a free state. When the hoop ring rotates at , the centrifugal force of the mirror plate presses the outer cylindrical the mirror plate) tightly against the hoop ring. Since the mirror plate a the clamping force, the rotating mirror has a very high dynamic preci- ther words, the surface precision of the mirror plate and the parallelism ective surfaces are basically without any variation during high speed

iving the rotating mirror: since the rotating mirror does not have a ft, the simplest driving method is to use a high-speed gas stream to op ring that fixes the mirror plate. The blade wheel of the dual-row

pneumatic turbine made of hard aluminum is connected to the hoop ring in a single piece by use of thermal shrink fitting. The blade wheel is driven by compressed air from the nozzle. The design method of the dual-row blade wheel and nozzle is basically the same as the design of the pneumatic rotating mirror mentioned above.

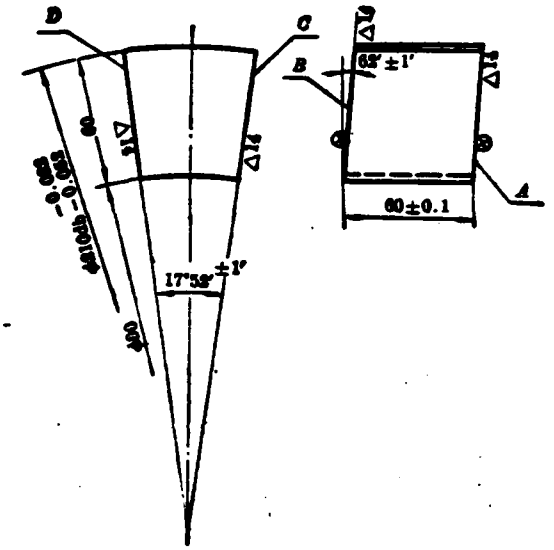

Fig. 6. Mirror plate of umbrella-shaped scan mirror:
Technical requirements:

1. The allowance of parallelism of A and B surfaces ≤5"
   $N_A=N_B=1/4$, $\Delta N_A=\Delta N_B=1/10$
   PIII
   ϕ coating of multiple layers of 1.06μ onto a total reflective film by use of an electron gun.
2. The allowance of the included angle between C and D surfaces ≤±1'
   $N_C=N_D=3$, $\Delta N_C=\Delta N_D=1/2$
3. All stepped difference≤1'
4. Group the 16 pieces of mirrors (8 pieces each for I and II with alternate arrangement) into a ring. Then process ϕ210 db outside the cylindrical surface and ϕ90 hole.

According to the compiled numbers, mirror plates are glued in sequence onto the inner wall of the hoop ring. A 1' angle meter is used to measure and calibrate the gluing precision. After the glue is dried by heat, the assembly is installed

on a special clamping fixture and dynamic equilibrium of the entire rotating mirror ring (including blade wheel) is calibrated; the required precision for dynamic equilibrium is less than 1 micron.

(C) Support of the rotating mirror: A support wheel props the outer cylindrical surface of the high-speed rotating mirror ring to solve difficulties due to the core-less shaft. The ratio between the diameter of the outer surface of the hoop ring and the diameter of the support wheel is 2:1. Four C100 ball bearings are used as props to the support wheel; the shaft of the ball bearing uses atomized oil as a lubricant. The processing precisions of support wheel, hoop ring and support seat can ensure the dynamic precision and stability of the high-speed rotating mirror. Two conical surfaces of the pressure wheel are used to restrain the axial-direction motion of the rotating mirror.

Figure 7 shows the exterior of the umbrella-shaped scan mirror (including air screening system).

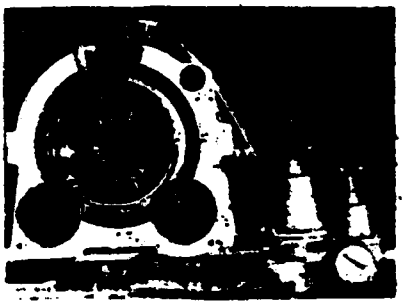

Fig. 7. Picture showing exterior of umbrella-shaped scan mirror.

III. Results and Discussion

(1) As proven by experimental results, these two types of rotating mirrors attained the pre-determined design indexes. By using the photoelectric speed measurement method, the rotating speed of the first rotating mirror is n≈40,000 r.p.m. and the speed of the second rotating mirror is n≈7500 r.p.m. The performances of these rotating mirrors give fast start, steady rotating speed, and dynamic equilibrium during rotation; these features meet the pre-determined purpose of scanning. Thus, the orientation of high energy laser output can be improved several times.

(2) The method of fixation of the mirror plate onto the umbrella-shaped rotating mirror is rational. During high-speed rotation, the mirror plates are only acted on by centrifugal force without appreciable deformation. The shearing and equal-thickness interference methods in experiments make dynamic and static measurements for the same mirror plate for comparison; the results prove that the wedge-shaped and surface type deformations are within the desirable allowance range. The effect of the scan and restoration of rotating mirror is satisfactory.

(3) Basically, the rotational speed of the pneumatic rotating mirror is determined by the design parameters of the turbine. As seen from the calculation formula in design, the theoretical speed of the gas flow at the outlet of the nozzle is

$$V=\sqrt{\frac{2K}{K-1}gRT_{*}\left[1-\left(\frac{P_{e}}{P_{*}}\right)^{\frac{K-1}{K}}\right]}$$

which is only related to the ratio between the inlet and outlet gas pressures, and is not related to the nozzle diameter. However, the nozzle diameter can directly affect turbine power; by properly increasing nozzle diameter, turbine power can be increased. Under the situation of higher resistance (such as bearing friction, air resistance and energy consumption due to vibration), the starting time can be shortened and the speed of the rotating mirror can be slightly increased. Of course, an oversized nozzle will considerably increase the gas consumption, and correspondingly affect the reduction of P_s.

As proven by experiments, the precision of dynamic equilibrium of the rotating mirror can directly affect its rotational speed. Rotating mirrors of the same structure may have a rotational speed considerably lower than the rated speed in design because of insufficient calibration of dynamic equilibrium.

(4) The compressed air used for gas-film bearing requires a high degree of dust, oil and humidity removal. Before the air enters the gas-film bearing, a set of air screening systems should be installed, including an oil-water separator, a pressure-regulating valve, a pressure gauge and a secondary screener. The function of the specially-designed secondary screener is to filter the compressed air after initial screening through a can of silicon glue and several layers of felt to

further remove tiny dust particles and water vapor in the air. The silicon glue and felt should be periodically dried and discarded.

(5) Figure 8 shows the scanning image (an arc shape) of the umbrella-shaped rotating mirror; the curvature of the arc is related to the diameter of the umbrella-shaped rotating mirror. The larger the diameter of the rotating mirror, the smaller is the curvature of the scan arc; the closer to the straight-line scan, the more can the magnifier be sufficiently utilized. However, the larger the diameter of the rotating mirror, the more complex is the manufacturing technique of the rotating mirror and the greater the difficulty in attaining the same scan precision. Therefore, a compromise between advantages and disadvantages should be made.

Fig. 8. Scan photograph of an umbrella-shaped rotating mirror.

(6) Noise problem: Silencers are installed at the exhaust openings of an air turbine for two types of rotating mirrors. However, the design of the silencer for the umbrella-shaped rotating mirror is not satisfactory; during operation, relatively loud noise is still heard.